Anatomo-functional correspondence in the voice-selective regions of human prefrontal cortex

Melina Cordeau, Ihsane Bichoutar, David Meunier, Kep Kee Loh, Isaure Michaud, Olivier A Coulon, Guillaume Auzias, Pascal Belin

Anatomo-functional correspondence in the voice-selective regions of human prefrontal cortex

Mélina Cordeau[1], Ihsane Bichoutar[2], David Meunier[1], Kep-Kee Loh[3,4], Isaure Michaud[1], Olivier Coulon[1,6], Guillaume Auzias[1], Pascal Belin[1,5,6]

[1] Institut de Neurosciences de la Timone, Aix Marseille Université, UMR 7289 CNRS, 13005, Marseille, France
[2] Institute of Neuroscience and Medicine (INM-1), Forschungszentrum Jülich, Jülich, Germany
[3] Montreal Neurological Institute, McGill University, Montreal, Quebec, Canada
[4] Department of Psychology, National University of Singapore, Singapore
[5] Psychology Department, Montreal University, C.P. 6128, succ. Centre-ville, Montreal, QC H3C 3J7, Canada
[6] Institute of Language Communication and the Brain, ILCB, Aix-en-Provence, France

Abstract

Group level analyses of functional regions involved in voice perception show evidence of 3 sets of bilateral voice-sensitive activations in the human prefrontal cortex, named the anterior, middle and posterior Frontal Voice Areas (FVAs). However, the relationship with the underlying sulcal anatomy, highly variable in this region, is still unknown. We examined the inter-individual variability of the FVAs in conjunction with the sulcal anatomy. To do so, anatomical and functional MRI scans from 74 subjects were analyzed to generate individual contrast maps of the FVAs and relate them to each subject's manually labeled prefrontal sulci. We report two major results. First, the frontal activations for the voice are significantly associated with the sulcal anatomy. Second, this correspondence with the sulcal anatomy at the individual level is a better predictor than coordinates in the MNI space. These findings offer new perspectives for the understanding of anatomical-functional correspondences in this complex cortical region. They also shed light on the importance of considering individual-specific variations in subject's anatomy.

Keywords: Human, fMRI, Voice perception, Individual variability, Sulcal anatomy

1. Introduction

The cerebral processing of voice information has been shown to involve several voice-selective cortical regions: the Temporal Voice Areas of bilateral secondary auditory cortex (Belin et al., 2000; Pernet et al., 2015) but also 3 bilateral regions of frontal cortex we called the Frontal Voice Areas (FVA; Aglieri et al., 2018). Based on group-averaged fMRI results, the anterior frontal voice area (aFVA) in the left hemisphere appears to correspond to the *pars orbitalis* of the inferior frontal gyrus (IFG) (Brodmann area BA 47) and in the right hemisphere to the *pars triangularis* of the IFG (BA 45); the middle frontal voice areas (mFVA) bilaterally correspond to the upper part of the *pars opercularis* of the IFG (BA 44); and the posterior frontal voice areas (pFVAs) to the precentral gyrus close to the junction with the middle frontal gyrus (BA 6). However, the localization of the FVAs seems much more variable at the individual participant level.

A portion of the inter-individual variability in the occurence and position of the FVAs could conceivably be related to the high inter-individual variability in the anatomy of prefrontal folding patterns. Detailed examination of prefrontal sulci such as the horizontal ascending ramus of the lateral fissure (Sprung-Much and Petrides, 2020), the ascending ramus of the lateral fissure or the diagonalis sulcus (Sprung-Much and Petrides, 2018), has uncovered strong variability in their existence and spatial organization. Indeed, correspondence between the localization of functional activations and local sulcal anatomy has been observed in multiple cases, such as for the position of the motor hand representation relative to the 'hand knob' of Central Sulcus (Sun et al., 2012), the relationship between cortical folding in the visual cortex and retinotopic maps (Rajimehr and Tootell, 2009), or the localization of the temporal voice areas relative to the 'Superior Temporal Asymmetrical Pit' of the Superior Temporal Sulcus (Bodin et al., 2018). One can also mention some anatomo-functional correspondances at the level of the lateral prefrontal cortex (Amiez et al., 2016, 2006; Amiez and Petrides, 2018; Zlatkina et al., 2016), the cingulate (Amiez et al., 2013; Amiez and Petrides, 2014), the orbitofrontal cortex (Li et al., 2015), the visual cortex (Benson et al., 2014, 2012; Weiner et al., 2018, 2014; Witthoft et al., 2014), as well as the lateral parietal cortex (Konen and Kastner, 2008; Tootell et al., 1997). We can also highlight a study (Lopez-Persem

et al., 2019) that showed that the sulcal organization is a better predictor than MNI coordinates to identify the functional organization of the ventromedial prefrontal cortex.

Here we address that question by examining at the individual subject-level the relative location of the FVAs and frontal sulci using anatomical and functional MRI data from 74 healthy adult participants (Figure 1). We assess (1) whether FVAs show consistent relationship to particular frontal sulci; and (2) whether these relationships could be more predictive of the location of a particular FVA than the group-average MNI coordinates.

We observe consistent associations between the FVAs and specific sulci. For the mFVAs and pFVAs, the distance to the associated sulcus is ~2-3 times shorter than the distance to the average MNI coordinate of that FVA.

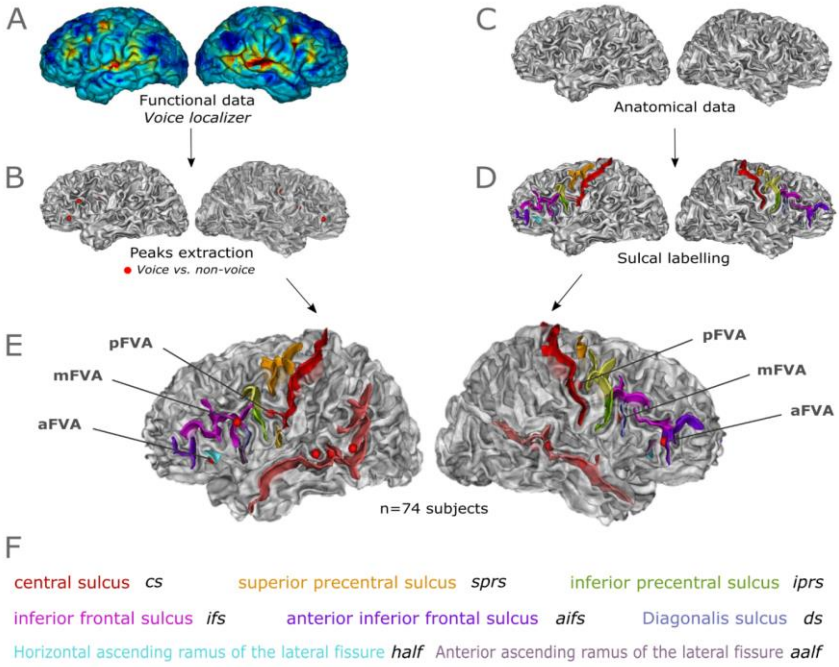

Figure 1: Summary of the methodology used to examine anatomo-functional correspondences between FVAs and frontal sulci at the individual level*. A. The functional map of the contrast Vocal sounds vs. Nonvocal sounds from the Voice Localizer is shown overlaid on the 3D cortical anatomy in one participant. B. Local voice selectivity maxima, individually extracted in search zones around the group-average locations of the FVAs, are represented as red spheres centered on each local maximum C. 3D mesh of the gray-white matter interface. D. Prefrontal sulci of interest were individually labeled. E. Anatomical and functional data are registered for computing the distance between sphere centers and sulci. F. Frontal sulcus nomenclature used and associated color code: Central sulcus (cs), superior precentral sulcus (sprs), inferior precentral sulcus (iprs), inferior frontal sulcus (ifs), anterior inferior frontal sulcus (aifs), anterior ascending ramus of the lateral fissure (aalf), horizontal ascending ramus of the lateral fissure (half), diagonalis sulcus (ds).*

2. Materials and methods

2.1 Participants

We scanned seventy-four (*n* = 74; 36 males and 38 females ; age (mean ± SD) = 38,5 ± 19,7) healthy adult volunteers on the localizer scan as part of experiments of the Voice Neurocognition Laboratory of the Institute of Neuroscience and Psychology at University of Glasgow. Participants were recruited from the population of Glasgow and were of various ethnic backgrounds, education and manual lateralization. Participants all provided written informed consent prior to participation, in accordance with the Declaration of Helsinki. The experiments were approved by the local ethics committee at University of Glasgow.

2.2 Voice localizer protocol and stimuli

The voice localizer consists of a ten minutes and twenty seconds-long block design with 40 eight seconds-long blocks of either vocal (20 blocks) or non-vocal (20 blocks) sounds from stimuli already used in Belin et al., 2000. Stimuli were presented using Media Control Functions (DigiVox, Montreal, Canada) via electrostatic headphones (NordicNeuroLab, Norway; or Sensimetrics, USA) at a comfortable level (80–85 dB SPL). The forty blocks are intermixed with twenty periods of silence allowing the hemodynamic to relax. Blocks consisted of a mixture of either vocal sounds or non-vocal sounds, with at most a 400 ms delay between consecutive stimuli. The order of blocks was attributed randomly and was similar for all participants. Vocal blocks contained only sounds of human vocal origin (excluding sounds without vocal fold vibration such as whistling or whispering) obtained from 47 speakers (7 babies, 12 adults, 23 children and 5 elderly people) and consisted of speech sounds (words, syllables or sentence extracts in different languages) and non-speech vocal sounds (emotional positive or negative sounds like laughs, sighs, or cries, and neutral sounds like coughs, and onomatopoeias). Non-vocal blocks consisted of natural sounds (from natural sources like falls, sea waves, wind, and from various animals like cats, dogs, lions, and elephants) and of man-made sources (from objects like cars, glass, alarms, and clocks, and from

(classical) musical pieces). Stimuli (16 bit, mono, 22,050 Hz sampling rate) were normalized for RMS (same normalization for all stimuli); a 1-kHz tone of similar energy is provided for calibration. Stimuli are available for download at: https://amubox.univ-amu.fr/s/edQWc7oSiaRNYsP.

2.3 MRI acquisitions

All scans were acquired on a 3T Siemens (Erlangen, Germany) Tim Trio scanner at the Centre for Cognitive Neuroimaging University of Glasgow. All fMRI data were acquired using a single-shot gradient-echo echo-planar imaging (EPI) sequence with the following parameters: field of view (FOV) = 210 × 210 mm^2, 32 slices per volume, interleaved slices order, voxel size 3 × 3 × 3.3 mm^3, acquisition matrix 70 × 70, flip angle = 77°, echo time (TE) = 30 ms. The repetition time (TR) was 2 s with an acquisition time (TA) of 2 seconds resulting in quasi-continuous scanning noise Participants were scanned while passively listening to the stimuli and keeping their eyes closed. For each participant, 310 EPI volumes were acquired together with a high-resolution 3D T1-weighted sagittal scan (voxel size 1mm^3 isotropic; acquisition matrix 256 256 192).

2.4 Preprocessing of anatomical data

T1w MRIs were processed using the Morphologist pipeline implemented in Brainvisa (Brainvisa 5.0.2 singularity version). This pipeline performed automatically T1 bias corrections, sulcus extraction and mesh generation. We then manually labeled the sulci of interest in the vicinity of the FVAs. We used the manual tool 'Anatomist show descriptive model' and the default nomenclature from Brainvisa, with modification of selected sulcus names to adopt the nomenclature of the Petrides atlas (Petrides, 2016). We labeled the central sulcus (cs), superior/inferior precentral sulcus (sprs/iprs), inferior frontal sulcus (ifs), diagonalis sulcus (ds), horizontal ascending ramus of the lateral fissure (half), anterior ascending ramus of the lateral fissure (aalf) and anterior inferior frontal sulcus (aifs - generated by brainvisa but in our study it might correspond to the sulci pretriangular sulcus (prts) combined with some other highly variable sulci in the petrides atlas). The labeling was performed in all 74 participants, with n=9 participants initially labeled

independently by 2 experimenters. The two experimenters are disagreed about the labeling of any sulcus only 5 times across the 9 participants (disagreed about one labeling of the aalf, 2 times about the ds, 1 times about the sprs and 1 time about the iprs); they are agreed (or disagreed with only one or two branch on the sulcus) in all the other cases i.e. 96% of the cases. This analysis confirmed the reliability of the labeling of the frontal sulcus for the 74 participants.

2.5 Preprocessing of functional data

SPM VERSION was used to preprocess functional data. We made a realignment of the 310 EPI volumes, T1w native image have been then coregistered to the mean of realigned EPIs through normalized mutual information, smoothing (6x6x6) of the mean of realigned EPIs, and T1 images were segmented into their native space tissue components (gray and white matter, and CSF). Next we computed an fMRI model estimation with the multiple conditions (names = VOCAL and NONVOCAL; duration = 8 and 8; onset = VOCAL [22 62 82 112 132 162 202 222 242 262 312 352 372 402 432 462 482 512 542 572], NONVOCAL[12 32 52 102 122 142 182 232 282 302 322 342 382 422 442 472 502 522 552 592]) and motion parameters determined during preprocessing as regressors of no interest.We then calculated for each individual subject its contrast map corresponding to the beta maps for VOCAL minus the beta map for NON-VOCAL. Voice-selective regions were identified as those showing a significantly greater activity for voice than for non-voice categories for each individual participant ($p$value < 0,001 uncorrected).

2.6 Definition of the search zone at the individual level

Six Frontal Voice Areas have been described by Aglieri et al., 2018 in prefrontal cortex based on the average activation maps from 90 DARTEL-registered participants. The coordinates in the MNI space of the average peaks are : aFVA left (-39 27 -3) and aFVA right (54 32 0) approximately corresponding to the location of the pars orbitalis/triangularis of the Inferior Frontal Gyrus, mFVA left (-48 16 21) and mFVA right (48 18 24) corresponding to the pars opercularis of the Inferior Frontal Gyrus , pFVA left (-52 -8 48) and pFVA right (51 -2 48) corresponding to the Precentral Gyrus. We choose to use these 6 average peaks to guide the

identification of the functional local maxima in each individual's native space. We considered those three locations in each hemisphere as the center of a limited search zone and we selected the peak of the voice vs. non-voice contrast in these regions – if one could be found. Two experimenters independently extracted individual FVAs in a sample of 15 participants to examine inter-rater agreement and refine the search strategy. The two experimenters agreed on the (x,y,z) coordinates and the nomenclature (anterior, middle or posterior FVA) in 52,2% of the cases (47/90 peaks); agreed on the (x,y,z) coordinates but not for the nomenclature in 36,7% of the cases (33/90 peaks); and disagreed with the coordinates in 11,1% of the case (10/90 peaks) with a mean difference (in mm) between the coordinates of (7, 19, 16). We made a second round of evaluation after corrections and we obtained 100% of agreement between coordinates and nomenclature for the two experimenters.

2.7 Co-registration functional on anatomical data

The coregistration between anatomy and function has been computed with Brainvisa. The referentials of both objects were placed in the same space (native anatomy) in order to visualize the spheres on the individual mesh of each subject. The aim of the sphere generation is to visually highlight local functional maxima and to describe the anatomical localization of them based on sulcal anatomy. These functional activations were also transformed in MNI space to determine the global localisation of the FVAs' cloud of points and to compare the accuracy of measurements in MNI space considering or not the sulcal anatomy.

2.8 Distance measurement between functional activations and the nearest sulci

To assess the anatomo-functional relationship between functional peaks and sulci, we performed distance measurements between the 8 frontal sulci of interest (central sulcus, superior-inferior precentral sulcus, inferior frontal sulcus, diagonalis sulcus, horizontal ascending ramus of the lateral fissure, anterior ascending ramus of the lateral fissure and anterior inferior frontal sulcus) and all the individual FVAs.

We manipulated the Brainvisa objects (functional spheres, meshes and sulci) using the Brainvisa 5.0.2 singularity version, and we performed an Euclidian distance estimation with Spicy (numpy/python).

3. Results

3.1. Individual occurrence of the Frontal Voice Areas

We first examined the occurrence at the individual level of the different FVAs in our sample of 74 participants. We report in Table 1 the proportion of participants in whom each of the FVAs could be observed or not, individually in the left and/or right hemispheres. The most commonly observed FVA was the pFVA that could be identified bilaterally in 37,9% of the sample. The anterior FVA was much less frequently observed, with an absence around 80% in the sample of 74 participants. Binomial tests conducted for each of the three FVAs confirmed that the distribution is statistically different from chance in the aFVAs, with many more participants in whom none could be found, and much fewer participants in whom it could be identified at all, than the expected 25%. The number of bilateral pFVAs was also significantly higher than the 25% proportion expected by chance.

%	Left	Right	Bilateral	none
aFVA	9 (12,2%)*	4 (5,4%)***	2 (2,7%)***	59 (79,7%)***
mFVA	11 (14,9%)	19 (25,7%)	24 (32,4%)	20 (27,0%)
pFVA	12 (16,2%)	12 (16,2%)	28 (37,9%)*	22 (29,7%)

Table 1: Individual occurrence of the FVAs.

*Each cell indicates, for each of the 3FVAs (rows), the number (and proportion) of participants in whom the FVA was identified in a single hemisphere (left or right), in both hemispheres (bilateral) or in none. Binomial tests with Bonferroni correction (α/3) were performed to identify deviations from chance distribution across the 4 cells. *:p<0,05 corr.; ***:pvalue<0,001 corr.*

3.2 Individual occurrence of the frontal sulci

In parallel we manually labeled and examined the individual occurrence of the main frontal sulci located around the FVAs. Table 2 indicates the proportion of participants in whom each of the main frontal sulci of interest were observed. Variability in occurrence concerned mostly the diagonalis sulcus (ds), the horizontal

ascending ramus of the lateral fissure (half) and the anterior ascending ramus of the lateral fissure (aalf), which were absent in several participants.

Sulci	Left	Right
Horizontal ascending ramus of the lateral fissure	90,5%	91,9%
Anterior ascending ramus of the lateral fissure	94,6%	97,3%
Diagonalis sulcus	62,2%	55,4%
Central sulcus	100%	100%
Inferior frontal sulcus	100%	100%
Anterior inferior frontal sulcus	100%	100%
Inferior precentral sulcus	100%	100%
Superior precentral sulcus	100%	100%

Table 2: Individual occurrence of the main prefrontal sulci

Cells indicate, for each sulcus of interest, the proportion of participants in which the sulcus is present in the left and right hemispheres.

3.3 Relationship between the FVAs and frontal sulci

Next, we assessed whether each FVA was located closer to a particular prefrontal sulcus than the others. Figure 2 indicates, for each of the 6 FVAs, the proportion of participants in whom the FVA was found closer to each of the main sulci of interest, in the individual (native) space. We found strong, symmetrical associations between each FVA and a particular sulcus. Bonferroni-corrected binomial tests confirmed that there were greater-than-chance associations between each FVA and a particular sulcus, symmetrically across hemispheres: the left and right aFVAs were significantly associated with the horizontal ascending ramus of the lateral fissure (half*)*; the left and right mFVAs were most often closest to the inferior frontal

sulcus (*ifs)* ; the left and right pFVAs were most often closest to the inferior precentral sulcus (*iprs)* (Fig 2).

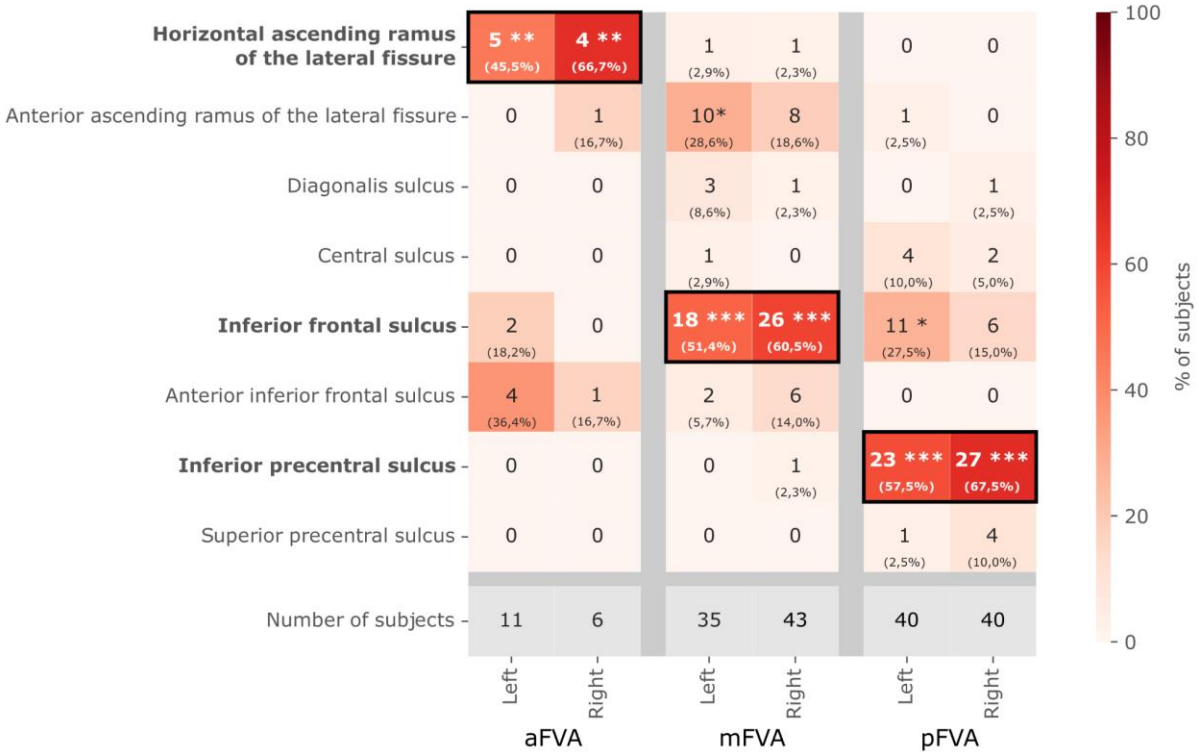

Figure 2: Association of FVAs with particular sulci

For each FVA (columns), cells indicate the number (and proportion) of participants in whom the FVA peak was closer to each sulcus of interest (rows). Stars indicate cells for which the proportion of participants is significantly above the 12.5% expected by chance as assessed by a Bonferroni-corrected Binomial test.:p<0,05 corr.; **:p<10^{-7} corr.; ***:p<10^{-12}corr. The bottom row in gray indicates the number of participants in whom each FVA was observed.*

3.4 Distance to sulcus vs. distance to average coordinate in the MNI space

Finally, we assessed whether the distance to the associated sulcus in the individual space was more predictive of each FVA localization than its distance to the average coordinate computed across individuals in the MNI space. Indeed, the location of FVAs was highly variable across individuals, resulting in widely spread peaks in MNI space (Fig 3a). Figure 3b shows, for each of the 6 FVAs, the distribution of distances to average MNI coordinate vs. the distance to associated sulcus, after transformation to MNI space, for normalization. For the aFVAs, median distances were smaller relative to the *half* sulcus than to the average MNI coordinates, but

not significantly (aFVA left pvalue=0,49; aFVA right pvalue=0,31). For the middle and posterior FVAs, the difference was stronger, and highly significant in both hemispheres (mFVA left pvalue=5,9.10^{-7}; mFVA right pvalue=2,8.10^{-8}; pFVA left pvalue=8,2.10^{-8}; pFVA right pvalue=6,1.10^{-8}). Non-parametric Wilcoxon tests were performed to compare two-by-two the medians and Bonferroni correction ($\alpha/3$) was applied. Median distances to MNI average are reported in table3.

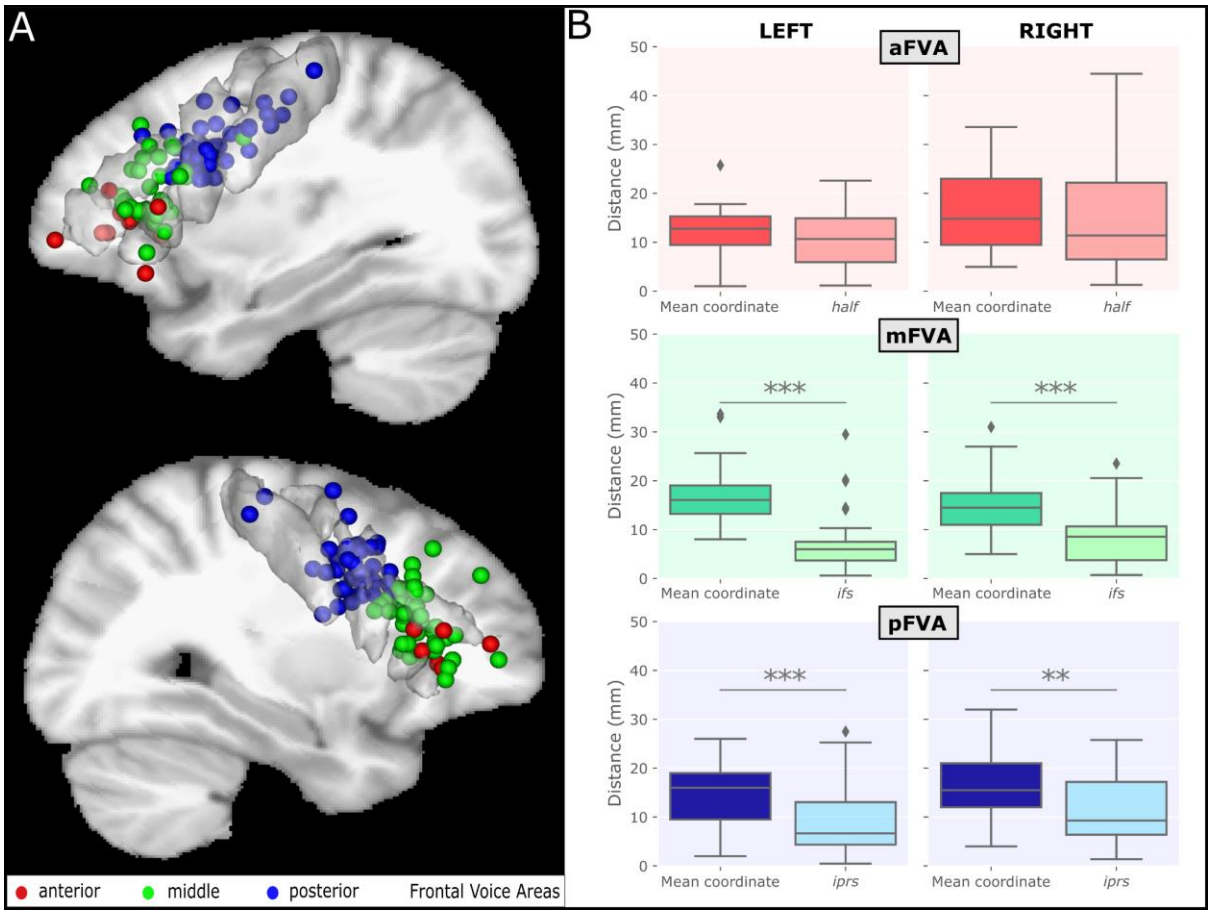

Figure 3: FVA spatial dispersion in functional vs. anatomical space

A. Dispersion of FVAs peaks from every individual are shown in MNI space. aFVAs are represented in red, mFVAs in green and pFVAs in blue.

*B. For each FVA, we show the distribution of the distances to the MNI average (left) vs. the distances to the associated sulcus from the same individual. Stars indicate significance of the difference as assessed by Wilcoxon's after Bonferroni correction: *:pvalue<0,05corr.; **:pvalue<0,01corr.; ***:pvalue<0,001corr.*

	LEFT		RIGHT	
	Median distance to mean coordinate	Median distance to sulcus	Median distance to mean coordinate	Median distance to sulcus
aFVA	11,0	8,6	10,6	4,4
mFVA	14,0	5,6	12,2	4,8
pFVA	12,9	2,9	11,4	4,2

Table 3: Median distances to MNI average

Cells indicate, for each boxplot represented in the fig.3, the median of distances between individual peaks and either group-level average or corresponding sulcus.

4. Discussion

We show here that there is a clear relationship between the functional localization of the Frontal Voice Areas and the sulcal anatomy of prefrontal sulci at the individual level. We also show that this sulcal anatomy can be more informative of an individual's FVA localization than average coordinates from group-level analysis.

4.1 Individual analysis reveals high inter-subject variability in both functional location of the FVAs and precise sulcal anatomy

In many participants we were able to identify at the individual level the FVAs previously described at the group level (Aglieri et al., 2018) (Table 1). This was particularly the case for the mFVA and pFVA that could be observed in at least one hemisphere in nearly three quareters of the participants, and in both hemispheres in about a third of the participants. The aFVA was much less frequently observed, however, seen in either hemisphere in only 1 subject out of 5 (Table 1). There was no clear hemispheric lateralization in this pattern, mirroring the bilateral and essentially symmetrical group-level FVAs. When observed, individual-level FVAs were also fairly variable in their localization, as shown in Fig. 3a.

Individual examination of sulcal anatomy in the inferior prefrontal region also revealed high variability, both in the shape of the sulci, as well as in the presence of some classical sulci (Table 2). The diagonalis sulcus, in particular, could be identified in a little more than half the participants, in line with previous studies.

4.2 Individual analysis reveals a relationship between the Frontal Voice Areas and prefrontal sulcal anatomy

Despite functional and anatomical variability, we observed a clear correspondence between anatomy and function. When they could be observed in either hemisphere, the aFVAs were found most often closest to the horizontal ascending ramus of the lateral fissure; the mFVAs closest to the inferior frontal sulcus; and the pFVAs closest to the inferior precentral sulcus.

Structure-function relationships have already been reported in the literature, for example the position of the motor hand representation relative to the 'hand knob' of Central Sulcus (Sun et al., 2012), or the localization of the temporal voice areas relative to the 'Superior Temporal Asymmetrical Pit' of the Superior Temporal Sulcus (Bodin et al., 2018). Other examples include K.Weiner's work on the functional implications around the fusiform gyrus (Weiner and Zilles, 2016), or Arcaco's buried gyral folds along the superior temporal sulcus in macaque lateral temporal cortex, which selectively predict the location of face-sensitive regions (Arcaro et al., 2020). Finally, we can mention the work of C. Amiez and M. Petrides on structure-function relations, such as the conditional visuomotor activity of the hand and the frontal eye field which are located in the superior precentral sulcus (Amiez et al., 2006). Our findings are consistent with these previous studies, and extend the notion of relationships between anatomy and function to the prefrontal cortex.

4.3 Individual anatomy can be more predictive of functional location than group-level average coordinates

We found that for the middle and posterior FVAs in both hemispheres, the distance between the functional peak and the associated sulcus was on average considerably smaller than its distance to the group-level average coordinate. The median distance between the mFVA and the inferior frontal sulcus was around 2 times smaller than to group-level mFVA average; median distance to inferior precentral sulcus was about 3 times smaller than to group average for the pFVAs (Figure 3, Table 3).

In contrast, for the most anterior FVAs, we did not find a significant difference between distance to the average coordinate and to the horizontal ascending ramus of the lateral fissure (*half*). Possible explanations for this could be: (1) lack of statistical power due to fact that individual aFVAs could only be observed in a very small number of participants (11 participants showed this activation in the left hemisphere and 6 in the right hemisphere); (2) the *half* is a highly variable sulcus that was often absent. Better characterizing the complexity of the sulcal

morphology of this region is crucial for understanding the role of functional activations in language-related studies (Sprung-Much and Petrides, 2020).

Thus, part of the functional variability observed in FVA localization seems to be explained by sulcal variability, and for the m and pFVAs, individual anatomical sulcation seems a better indicator of function localization than the barycenter of a rather spread out point cloud. This observation is in line with previous studies such as (Rivière et al., 2022) and (Coalson et al., 2018) that showed that spatial normalization is not optimal for dealing with inter-subject variability in cortical morphology.

4.4 Functional roles of the three FVAs based on sulcal anatomy

Here, we discuss the potential functional role of each FVA in voice processing based on their sulcal locations.

4.4.1 aFVA – Retrieval and integration of semantic and auditory aspects of voice information to drive vocal actions

The aFVA is most closely associated with the *half,* which separates the ventral part of *pars triangularis (area 45)* from *pars orbitalis (area 47/12)* in the anteriormost part of the inferior frontal gyrus (Sprung-Much and Petrides, 2020). It is also located near to the *anterior ifs*, which corresponds to the region around the *prts* in Petrides 2019 ("Atlas of the Morphology of the Human Cerebral Cortex on the Average MNI Brain - 1st Edition," book), where area 45 transits anteriorly into area 47/12 (Petrides and Pandya, 2002). Last, it is also related to the *aalf,* which forms the caudal border of area 45, with area 44 located posteriorly (Sprung-Much and Petrides, 2020). As such, we propose that aFVA is likely located in the anterior part of Broca's speech region (Broca, 1863), and could lie at the transition between cytoarchitectonic areas 45 and 47/12.

This region has access to: 1) higher-order processed semantic and multimodal inputs from the anterior and middle parts of the temporal lobe via the extreme capsule frontal-temporal fasciculus (Frey et al., 2008; Petrides and Pandya, 2009, 1988), which constitutes the *ventral speech pathway* (Hickok and Poeppel, 2007) ;

2) auditory inputs from the posterior superior temporal cortex via the arcuate fasciculus (Frey et al., 2014) ; 3) speech motor output areas, such as area 44 and the ventral premotor areas, which are located immediately posterior to the aFVA. This connectivity suggests that the aFVA would have a role in retrieving and integrating both the higher-order semantic and lower-order auditory aspects of voice information, to drive speech motor actions via the posterior inferior frontal cortex. Indeed, (Loh et al., 2020) demonstrated activations in this very area as participants were actively selecting between vocal actions based on vocal/verbal feedback. This role is likely preserved in non-human primates considering that the connectivity of area 45 is homologous across humans and monkeys (Loh et al., 2017).

4.4.2 mFVA – High-level control of orofacial-vocal motor actions based on phonological aspects of voice information

Our results indicated that the mFVA is most often found close to the *ifs,* at the more posterior part of the inferior frontal cortex (i.e. close to the *aalf, ds*) relative to the aFVA. The main neighbouring sulci of the mFVA form the boundaries of area 44 of the *pars opercularis* with *ifs* dorsally, *aalf* anteriorly, and *iprs* posteriorly, while the *ds* is known to be an axial sulcus within area 44 (Loh et al., 2020; Sprung-Much and Petrides, 2018). However, notably, in some participants, the mFVA extends into the area 45 territory (i.e. near to *half* and *ifs-a*). We propose that mFVA occupies *pars opercularis*, i.e. area 44.

In both humans and monkeys, this region connects to the posterior superior temporal cortex via the *arcuate fasciculus* (reviewed in (Becker et al., 2021)), and to the supermarginal gyrus via the *superior longitudinal fasciculus III.* This network constitutes the dorsal speech pathway (Hickok and Poeppel, 2007) which is implicated in phonological processing of speech. Apart from having access to temporal phonological inputs, area 44 (where mFVA is located) is strongly associated with the speech motor output region in ventral premotor cortex (Petrides, 2016). As such, functionally, the mFVA would be involved in the processing of phonological aspects of voice (obtained from the posterior temporal cortex) to regulate the control over speech/vocal motor production via the ventral

premotor area. Congruent with this role, area 44 has been shown to be involved in both the conditional selection of orofacial and vocal motor acts, as well as the active processing of vocal and verbal information (Loh et al., 2020). In nonhuman primates, area 44 has also been demonstrated to be involved in auditory-driven vocal motor control *(Aboitiz, 2018; Hage and Nieder, 2013).*

4.4.3 pFVA – Top-down influence on speech vocal perception

The pFVA is consistently located close to the *iprs,* which delimits area 44 anteriorly and ventral premotor area 6 posteriorly. It is sometimes found close to the *cs*, where the primary motor area 4 is found, and close to the *ifs*, which separates the middle frontal gyrus dorsally from the inferior frontal gyrus. Based on these neighboring sulci, the pFVA is situated in ventral premotor area 6 at the most caudal part of the inferior frontal cortex. The speech motor representations have been located in this region (Conant et al., 2014; Penfield and Rasmussen, 1950). Recent work (Real et al., 2017) reported that the ventral premotor area might contribute to the top-down perception of speech by generating feedforward predictive models of speech motor plans which are then compared with perceived auditory-vocal inputs in the temporal cortex. Ventral premotor cortex is anatomically connected to the posterior parietal and temporal cortices and is considered part of the dorsal speech pathway described by Hickok and Poeppel (Hickok and Poeppel, 2007). As such, the pFVA's role in voice processing would be in exerting a top-down influence on speech-vocal perception.

We can observe that these functional activations found in the human prefrontal cortex (FVAs) are also found in the frontal lobe of the macaques. To date, no study has demonstrated functional homology of these activations between the two species. Only the anterior activation of the temporal lobe (aTVA) has been described as functionally homologous between the two species (Clémentine Bodin et al., 2021). Therefore, it would be interesting to investigate whether functional homology exists in the frontal lobe and to examine whether the activations in monkeys, like humans, are associated with sulcal anatomy. Furthermore, we can

explore to what extent we can hypothesize about the evolution of voice perception between the two species.

4.5 Limitations and perspectives

Several limitations to our study must be considered. One is that we used an Euclidean distance in 3D for our comparisons. Given the pronounced folding of the cortical surface, a geodesic distance on the cortical surface (Le Troter et al., 2012) might have been more appropriate. Hausdorff (Huttenlocher et al., 1993) or Dice (Shamir et al., 2018) could be used in our case. However, Dice is a measure of overlap, which means it relies on delineating both the sulcus and the extent of activation (which is somewhat arbitrary). On the other hand, Hausdorff distance would allow us to compute a metric with respect to all parts of the sulcus instead of the nearest point. Since sulci are complex and variable structures, the interpretation of the Hausdorff distance would then be difficult, with for instance normalization issues relative to the variations in the size of the sulcus across individuals. Computing the Euclidean distance between the peak of activation and the nearest point from each sulcus has the advantages to avoid the thresholding effect from the Dice, and the normalization issue from the Hausdorff distance. In future work, we will consider other metrics and features of the cortical anatomy such as the sulcal pits (Auzias et al., 2015) and the 'plis de passage' (C. Bodin et al., 2021). We will also refine and clarify the anatomical characterization of morphological patterns of the sulci (such as Sprung-Much and Petrides, 2018), search for relationship with the depth of the sulcus (Bodin et al., 2018), or assess specifically the morphological variability of prefrontal sulci and a possible match with function as in (Sun et al., 2012). Another direction for future studies could be to seek to establish correspondences between the different names of sulci provided by various atlases.

Conflicts of interest

None.

Acknowledgments

This work was funded by Fondation pour la Recherche Medicale (AJE201214 to Pascal Belin and FDT202204015255 to Mélina Cordeau); Agence Nationale de la Recherche grants ANR-16-CE37-0011-01 (PRIMAVOICE), ANR-16-CONV-0002 (Institute for Language, Communication and the Brain), and ANR-11-LABX-0036 (Brain and Language Research Institute); the Excellence Initiative of Aix-Marseille University (A*MIDEX); and the European Research Council (ERC) under the European Union's Horizon 2020 research and innovation program (grant agreement no. 788240).

Credit author statement

Mélina Cordeau: Conceptualization, methodology, analysis, writing, visualization, project administration, funding acquisition **Ihsane Bichoutar**: analysis **David Meunier**: methodology **Kep-Kee Loh**: analysis, validation, writing **Isaure Michaud**: conceptualization, analysis **Olivier Coulon**: conceptualization, supervision, validation **Guillaume Auzias**: conceptualization, methodology, supervision, writing, validation **Pascal Belin**: conceptualization, supervision, writing, validation, project administration, resources, funding acquisition

References

Aglieri V, Chaminade T, Takerkart S, Belin P. 2018. Functional connectivity within the voice perception network and its behavioural relevance. *NeuroImage* **183**:356–365. doi:10.1016/j.neuroimage.2018.08.011

Amiez C, Kostopoulos P, Champod A-S, Petrides M. 2006. Local morphology predicts functional organization of the dorsal premotor region in the human brain. *J Neurosci* **26**:2724–2731.

Amiez C, Neveu R, Warrot D, Petrides M, Knoblauch K, Procyk E. 2013. The location of feedback-related activity in the midcingulate cortex is predicted by local morphology. *J Neurosci* **33**:2217–2228.

Amiez C, Petrides M. 2018. Functional rostro-caudal gradient in the human posterior lateral frontal cortex. *Brain Struct Funct* **223**:1487–1499.

Amiez C, Petrides M. 2014. Neuroimaging Evidence of the Anatomo-Functional Organization of the Human Cingulate Motor Areas. *Cereb Cortex* **24**:563–578. doi:10.1093/cercor/bhs329

Amiez C, Wutte MG, Faillenot I, Petrides M, Burle B, Procyk E. 2016. Single subject analyses reveal consistent recruitment of frontal operculum in performance monitoring. *Neuroimage* **133**:266–278.

Arcaro MJ, Mautz T, Berezovskii VK, Livingstone MS. 2020. Anatomical correlates of face patches in macaque inferotemporal cortex. *Proc Natl Acad Sci* **117**:32667–32678. doi:10.1073/pnas.2018780117

Atlas of the Morphology of the Human Cerebral Cortex on the Average MNI Brain - 1st Edition. n.d. https://shop.elsevier.com/books/atlas-of-the-morphology-of-the-human-cerebral-cortex-on-the-average-mni-brain/mcmanus/978-0-12-800932-1

Auzias G, Brun L, Deruelle C, Coulon O. 2015. Deep sulcal landmarks: Algorithmic and conceptual improvements in the definition and extraction of sulcal pits. *NeuroImage* **111**:12–25. doi:10.1016/j.neuroimage.2015.02.008

Becker Y, Loh KK, Coulon O, Meguerditchian A. 2021. The Arcuate Fasciculus and language origins: Disentangling existing conceptions that influence evolutionary accounts. *Neurosci Biobehav Rev*.

Belin P, Zatorre RJ, Lafaille P, Ahad P, Pike B. 2000. Voice-selective areas in human auditory cortex. *Nature* **403**:309–312. doi:10.1038/35002078

Benson NC, Butt OH, Brainard DH, Aguirre GK. 2014. Correction of Distortion in Flattened Representations of the Cortical Surface Allows Prediction of V1-V3 Functional Organization from Anatomy. *PLOS Comput Biol* **10**:e1003538. doi:10.1371/journal.pcbi.1003538

Benson NC, Butt OH, Datta R, Radoeva PD, Brainard DH, Aguirre GK. 2012. The Retinotopic Organization of Striate Cortex Is Well Predicted by Surface Topology. *Curr Biol* **22**:2081–2085. doi:10.1016/j.cub.2012.09.014

Bodin C., Pron A, Le Mao M, Régis J, Belin P, Coulon O. 2021. Plis de passage in the superior temporal sulcus: Morphology and local connectivity. *NeuroImage* **225**:117513. doi:10.1016/j.neuroimage.2020.117513

Bodin C, Takerkart S, Belin P, Coulon O. 2018. Anatomo-functional correspondence in the superior temporal sulcus. *Brain Struct Funct* **223**:221–232. doi:10.1007/s00429-017-1483-2

Bodin Clémentine, Trapeau R, Nazarian B, Sein J, Degiovanni X, Baurberg J, Rapha E, Renaud L, Giordano BL, Belin P. 2021. Functionally homologous representation of vocalizations in the auditory cortex of humans and macaques. *Curr Biol* **31**:4839-4844.e4. doi:10.1016/j.cub.2021.08.043

Broca P. 1863. Localization of cerebral functions. Location of articulate language. *Bull Soc Anthropol* **4**:200–203.

Coalson TS, Van Essen DC, Glasser MF. 2018. The impact of traditional neuroimaging

methods on the spatial localization of cortical areas. *Proc Natl Acad Sci* **115**. doi:10.1073/pnas.1801582115

Conant D, Bouchard KE, Chang EF. 2014. Speech map in the human ventral sensory-motor cortex. *Curr Opin Neurobiol*, Neural maps **24**:63–67. doi:10.1016/j.conb.2013.08.015

Frey S, Campbell JSW, Pike GB, Petrides M. 2008. Dissociating the Human Language Pathways with High Angular Resolution Diffusion Fiber Tractography. *J Neurosci* **28**:11435–11444. doi:10.1523/JNEUROSCI.2388-08.2008

Frey S, Mackey S, Petrides M. 2014. Cortico-cortical connections of areas 44 and 45B in the macaque monkey. *Brain Lang*, Neural Basis of Aspects of Language Processing **131**:36–55. doi:10.1016/j.bandl.2013.05.005

Hickok G, Poeppel D. 2007. The cortical organization of speech processing. *Nat Rev Neurosci* **8**:393–402. doi:10.1038/nrn2113

Huttenlocher DP, Klanderman GA, Rucklidge WJ. 1993. Comparing images using the Hausdorff distance. *IEEE Trans Pattern Anal Mach Intell* **15**:850–863. doi:10.1109/34.232073

Konen CS, Kastner S. 2008. Representation of Eye Movements and Stimulus Motion in Topographically Organized Areas of Human Posterior Parietal Cortex. *J Neurosci* **28**:8361–8375. doi:10.1523/JNEUROSCI.1930-08.2008

Le Troter A, Auzias G, Coulon O. 2012. Automatic sulcal line extraction on cortical surfaces using geodesic path density maps. *NeuroImage* **61**:941–949. doi:10.1016/j.neuroimage.2012.04.021

Li Y, Sescousse G, Amiez C, Dreher J-C. 2015. Local Morphology Predicts Functional Organization of Experienced Value Signals in the Human Orbitofrontal Cortex. *J Neurosci* **35**:1648–1658. doi:10.1523/JNEUROSCI.3058-14.2015

Loh KK, Petrides M, Hopkins WD, Procyk E, Amiez C. 2017. Cognitive control of vocalizations in the primate ventrolateral-dorsomedial frontal (VLF-DMF) brain network. *Neurosci Biobehav Rev*, An overview of nonhuman primates' communication and social abilities through behavioral and neuroscientific approaches **82**:32–44. doi:10.1016/j.neubiorev.2016.12.001

Loh KK, Procyk E, Neveu R, Lamberton F, Hopkins WD, Petrides M, Amiez C. 2020. Cognitive control of orofacial motor and vocal responses in the ventrolateral and dorsomedial human frontal cortex. *Proc Natl Acad Sci* **117**:4994–5005. doi:10.1073/pnas.1916459117

Lopez-Persem A, Verhagen L, Amiez C, Petrides M, Sallet J. 2019. The Human Ventromedial Prefrontal Cortex: Sulcal Morphology and Its Influence on Functional Organization. *J Neurosci* **39**:3627–3639. doi:10.1523/JNEUROSCI.2060-18.2019

Penfield W, Rasmussen T. 1950. The cerebral cortex of man; a clinical study of localization of function, The cerebral cortex of man; a clinical study of localization of function. Oxford, England: Macmillan.

Pernet CR, McAleer P, Latinus M, Gorgolewski KJ, Charest I, Bestelmeyer PEG, Watson RH, Fleming D, Crabbe F, Valdes-Sosa M, Belin P. 2015. The human voice areas: Spatial organization and inter-individual variability in temporal and extra-temporal cortices. *Neuroimage* **119**:164–174. doi:10.1016/j.neuroimage.2015.06.050

Petrides M. 2016. Chapter 3 - The Ventrolateral Frontal Region In: Hickok G, Small SL, editors. Neurobiology of Language. San Diego: Academic Press. pp. 25–33. doi:10.1016/B978-0-12-407794-2.00003-1

Petrides M, Pandya DN. 2009. Distinct Parietal and Temporal Pathways to the Homologues of Broca's Area in the Monkey. *PLOS Biol* **7**:e1000170. doi:10.1371/journal.pbio.1000170

Petrides M, Pandya DN. 2002. Comparative cytoarchitectonic analysis of the human and the macaque ventrolateral prefrontal cortex and corticocortical connection patterns in the monkey. *Eur J Neurosci* **16**:291–310. doi:10.1046/j.1460-9568.2001.02090.x

Petrides M, Pandya DN. 1988. Association fiber pathways to the frontal cortex from the superior temporal region in the rhesus monkey. *J Comp Neurol* **273**:52–66. doi:10.1002/cne.902730106

582 Rajimehr R, Tootell RBH. 2009. Does Retinotopy Influence Cortical Folding in Primate Visual
583 Cortex? *J Neurosci* **29**:11149–11152. doi:10.1523/JNEUROSCI.1835-09.2009
584 Real E, Asari H, Gollisch T, Meister M. 2017. Neural Circuit Inference from Function to
585 Structure. *Curr Biol* **27**:189–198. doi:10.1016/j.cub.2016.11.040
586 Rivière D, Leprince Y, Labra N, Vindas N, Foubet O, Cagna B, Loh KK, Hopkins W, Balzeau
587 A, Mancip M, Lebenberg J, Cointepas Y, Coulon O, Mangin J-F. 2022. Browsing
588 Multiple Subjects When the Atlas Adaptation Cannot Be Achieved via a Warping
589 Strategy. *Front Neuroinformatics* **16**.
590 Shamir RR, Duchin Y, Kim J, Sapiro G, Harel N. 2018. Continuous Dice Coefficient: a
591 Method for Evaluating Probabilistic Segmentations (preprint). Bioengineering.
592 doi:10.1101/306977
593 Sprung-Much T, Petrides M. 2020. Morphology and Spatial Probability Maps of the
594 Horizontal Ascending Ramus of the Lateral Fissure. *Cereb Cortex* **30**:1586–1602.
595 doi:10.1093/cercor/bhz189
596 Sprung-Much T, Petrides M. 2018. Morphological patterns and spatial probability maps of
597 two defining sulci of the posterior ventrolateral frontal cortex of the human brain: the
598 sulcus diagonalis and the anterior ascending ramus of the lateral fissure. *Brain Struct*
599 *Funct* **223**:4125–4152. doi:10.1007/s00429-018-1733-y
600 Sun ZY, Klöppel S, Rivière D, Perrot M, Frackowiak R, Siebner H, Mangin J-F. 2012. The
601 effect of handedness on the shape of the central sulcus. *NeuroImage* **60**:332–339.
602 doi:10.1016/j.neuroimage.2011.12.050
603 Tootell RBH, Mendola JD, Hadjikhani NK, Ledden PJ, Liu AK, Reppas JB, Sereno MI, Dale
604 AM. 1997. Functional Analysis of V3A and Related Areas in Human Visual Cortex. *J*
605 *Neurosci* **17**:7060–7078. doi:10.1523/JNEUROSCI.17-18-07060.1997
606 Weiner KS, Golarai G, Caspers J, Chuapoco MR, Mohlberg H, Zilles K, Amunts K, Grill-
607 Spector K. 2014. The mid-fusiform sulcus: A landmark identifying both
608 cytoarchitectonic and functional divisions of human ventral temporal cortex.
609 *NeuroImage* **84**:453–465. doi:10.1016/j.neuroimage.2013.08.068
610 Weiner KS, Natu VS, Grill-Spector K. 2018. On object selectivity and the anatomy of the
611 human fusiform gyrus. *NeuroImage* **173**:604–609.
612 doi:10.1016/j.neuroimage.2018.02.040
613 Weiner KS, Zilles K. 2016. The anatomical and functional specialization of the fusiform
614 gyrus. *Neuropsychologia*, Special Issue: Functional Selectivity in Perceptual and
615 Cognitive Systems - A Tribute to Shlomo Bentin (1946-2012) **83**:48–62.
616 doi:10.1016/j.neuropsychologia.2015.06.033
617 Witthoft N, Nguyen ML, Golarai G, LaRocque KF, Liberman A, Smith ME, Grill-Spector K.
618 2014. Where Is Human V4? Predicting the Location of hV4 and VO1 from Cortical
619 Folding. *Cereb Cortex* **24**:2401–2408. doi:10.1093/cercor/bht092
620 Zlatkina V, Amiez C, Petrides M. 2016. The postcentral sulcal complex and the transverse
621 postcentral sulcus and their relation to sensorimotor functional organization. *Eur J*
622 *Neurosci* **43**:1268–1283. doi:10.1111/ejn.13049
623

624

A. Appendices

A.1 Table: Percentage of simultaneous occurrence of each FVA in the same hemisphere

LEFT	**aFVA**	**mFVA**	**pFVA**
aFVA	-	6,8	6,8
mFVA	-	-	29,7
pFVA	-	-	-
RIGHT	aFVA	mFVA	pFVA
aFVA	-	4,1	4,1
mFVA	-	-	41,9
pFVA	-	-	-

For each hemisphere of the 74 participants, we looked at which FVA and in what proportion they were co-activated. For each of these left and right FVA we looked at whether or not they appeared simultaneously. We found that in both hemispheres, mFVA is often activated simultaneously with pFVA (29,7% in the left hemisphere, and 41,9% in the right hemisphere).

A.2 Table: Number of activations detected in each hemisphere

	LEFT	RIGHT
0 FVA	24,3	27,0
1 FVA	**37,8***	28,4
2 FVAs	35,1	**41,9***
3 FVAs	2,7	2,7

*Percentage of cases for which there are 0, 1, 2 or 3 activations in the left and right hemisphere separately (n=74 participants). We computed inverse binomial tests (2 tests, one for each hemisphere) and a Bonferroni correction (α/2) to know if some patterns of activations are significant in the population level. *: pvalue < 0,05 corrected. Beyond the positioning of the functional peaks (a, m, p) we asked ourselves which activation number (0, 1, 2 or 3) is most represented (tab. 3). These were 1 FVA in the left hemisphere (37,8% each), and 2 FVAs in the right hemisphere (41,9%). We made inferential statistics on these data to know if the number of FVAs in each hemisphere is higher than the level of chance: we performed a binomial test on both hemispheres and a Bonferroni correction (α/2) to know if these results are significant at the population level and we found that 1 FVA in left hemisphere and 2 FVAs in right hemisphere appears more often than the chance level (pvalue < 0,05 corr.).*

A.3 Table: Different activation patterns observed

		RIGHT			
		0 FVA	**1 FVA**	**2 FVAs**	**3 FVAs**
LEFT	**0 FVA**	12,2	6,8	5,4	0
	1 FVA	8,1	13,5	14,9	1,4
	2 FVAs	6,8	8,1	**20,3*** **	0
	3 FVAs	0	0	1,4	1,4

*Percentage of cases for which there are 0, 1, 2 or 3 activations in the left and right hemisphere simultaneously (n=74 participants). We computed an inverse binomial test and Bonferroni correction (α/16) to assess whether some patterns of activations were significant in the population level. ***: pvalue < 0,001 corrected*
We also confronted each of our patterns (0, 1, 2 or 3 activations) with the same possibilities in the other hemisphere, to see if we can establish a global pattern of activations (tab. 4). We noticed that the most represented pattern is 2 activations in the left hemisphere and 2 activations in the right hemisphere (20,3%). We performed an inverse binomial test and a Bonferroni correction (α/16) to know if the results are significant, and we found that 1 pattern appear significantly: 2 FVAs in both hemispheres is the pattern most commonly found (20,3%).

A.4 Figure: Distance between sulci of interest and the different Frontal Voice Areas

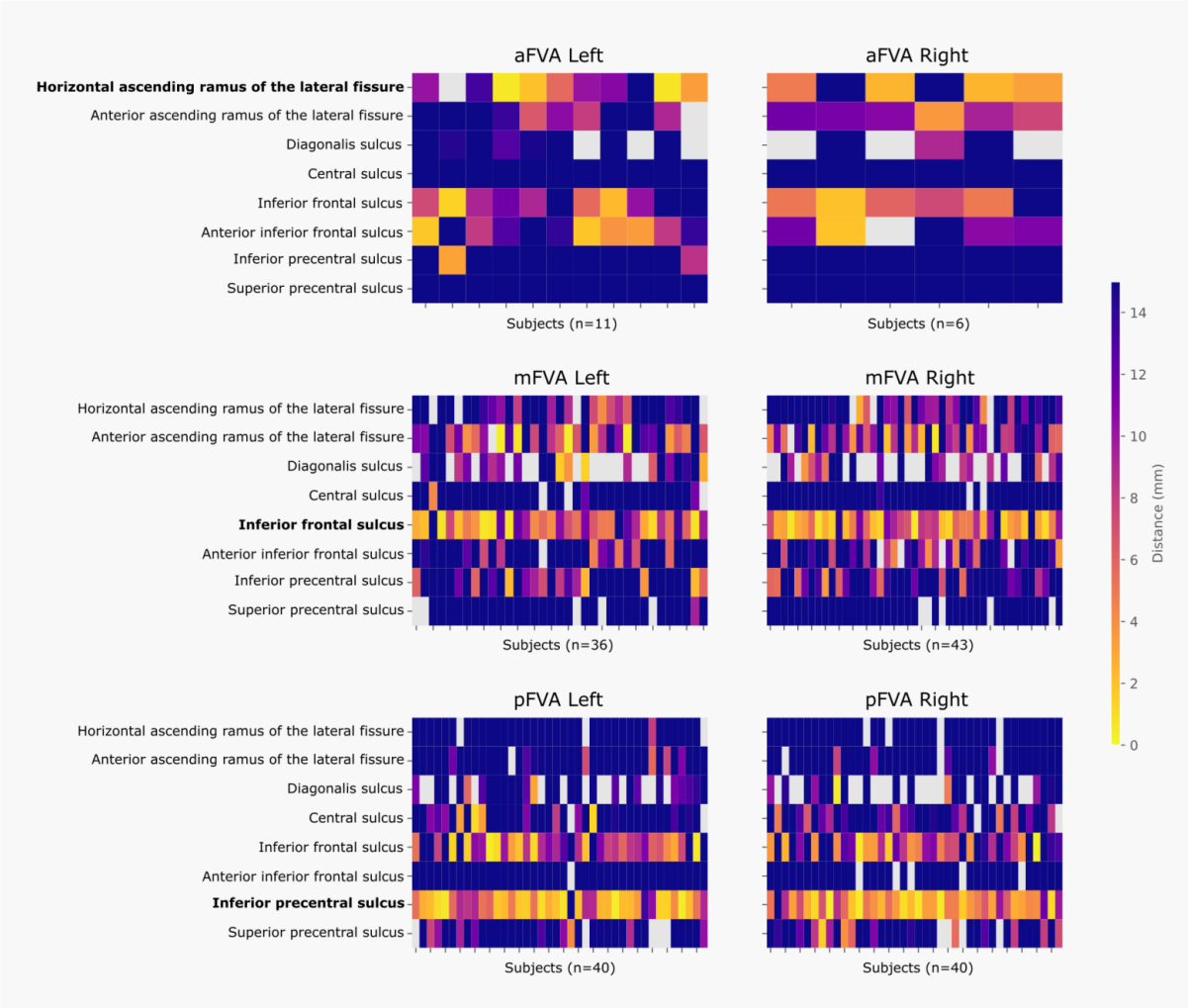

For each FVA, anterior (aFVA) middle (mFVA) and posterior (pFVA), we measure the distance (mm) to all the 8 sulci of interest, and we plot results on 6 heatmaps. Nearest sulci appear brighter.

Distance measurement between functional activations and the nearest sulcus – In addition to the information given by the nearest sulcus to the FVAs, we measured the distance between the functional peaks and all sulci of interest. This study allowed us to assessprecisely the organization of the sulci around the functional activation.

A.5 Figure: Examples of individual subjects displaying 0 activation or the 1, 2 or 3 FVAs

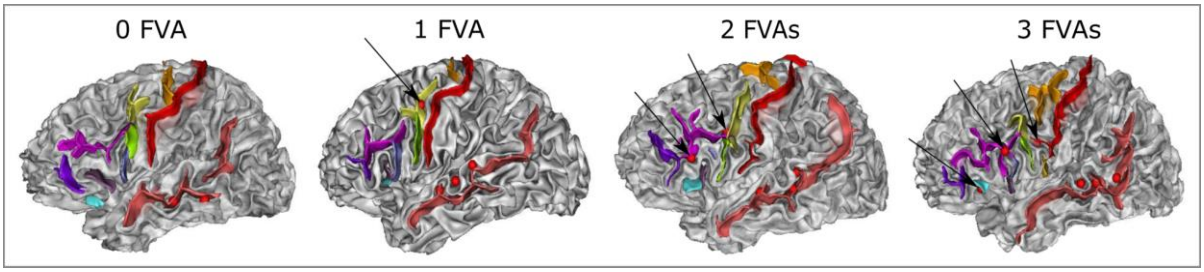

For each of the 74 subjects, a significant amount of anatomical and functional variability was observed. Here, we present 4 subjects that represent the 4 different activation patterns: either 0 activation, 1, 2, or 3 FVAs.